Available online at www.sciencedirect.com
SCIENCE DIRECT®
Coordination Chemistry Reviews 249 (2005) 1501–1510
COORDINATION CHEMISTRY REVIEWS
www.elsevier.com/locate/ccr

Review

Excimer and electron transfer quenching studies of a cyclometalated platinum complex

Biwu Ma [a], Peter I. Djurovich [b], Mark E. Thompson [a, b, *]

[a] *University of Southern California, Department of Materials Science, Los Angeles, CA 90089, USA*
[b] *University of Southern California, Department of Chemistry, 840 Downey Way, Los Angeles, CA 90089, USA*

Received 20 June 2004; accepted 6 February 2005
Available online 5 April 2005

Abstract

Luminescence quenching studies of a cyclometalated complex, platinum(II) (2-(4′,6′-difluorophenyl)pyridinato-$N,C^{2'}$)(2,4-pentanedionato-O,O) (**FPt**), in solution at room temperature are reported. The **FPt** complex undergoes efficient self-quenching in solution at room temperature that can be successfully modeled by a monomer/excimer phosphorescence mechanism with a diffusion limited rate constant ($4.2 \pm 0.3 \times 10^9\ M^{-1}\ s^{-1}$). The emission lifetimes for **FPt** monomer and excimer in 2-methyltetrahydrofuran at room temperature are 330 ns (±15 ns) and 135 ns (±10 ns), respectively. The excited state properties of **FPt** were also investigated. A triplet energy E_T of 2.8 eV and excited-state reduction potential $E(FPt^{*/-})$ of 0.81 V versus SCE were determined from quenching studies in agreement with values estimated from emission spectra and a thermochemical cycle. The excited-state oxidation potential $E(FPt^{*/+})$ cannot be determined from electrochemical data since **FPt** undergoes irreversible oxidation. However, a value of $E(FPt^{*/+}) = -1.41$ V versus SCE was established from an electron transfer quenching study and thus, a ground state oxidation potential for **FPt** can be estimated to be 1.30 V versus SCE.

Keywords: Quenching; Platinum complex; Excimer; Energy transfer; Electron transfer; OLEDs

* Corresponding author. Tel.: +1 213 740 6402; fax: +1 213 740 8594.
E-mail address: met@usc.edu (M.E. Thompson).

0010-8545/$ – see front matter © 2005 Elsevier B.V. All rights reserved.
doi:10.1016/j.ccr.2005.02.004

1. Introduction

Square planar platinum complexes have attracted considerable interest for their potential use in a wide range of applications such as optical chemosensors [1], photocatalysis [2], and molecular photochemical devices for solar energy conversion [3]. Platinum complexes have also been applied successfully as phosphorescent emitters in organic light-emitting diodes (OLEDs) [4]. OLEDs fabricated with platinum complexes can exhibit high emission efficiency, as the strong spin-orbital coupling of platinum allows for efficient phosphorescence at room temperature [5]. Efficient phosphorescent dopants are important components in OLEDs since the hole–electron recombination process leads to a mixture of singlet and triplet excited states in the device [6]. Recently, white OLEDs have been prepared with an organometallic Pt complex, platinum(II) (2-(4′,6′-difluorophenyl)pyridinato-$N,C^{2'}$)(2,4-pentanedionato-O,O) (**FPt**), with emission that originates from both isolated Pt complexes and excimers or aggregates of the same complex [7]. The devices utilized a very simple device structure since only a single dopant is used in the emissive layer and were highly efficient. In order to better understand the excited state properties of **FPt**, we have carried out an extensive photophysical quenching study of this complex and report it herein.

Self-quenching of platinum complexes has been well known since Che and co-workers reported concentration dependence of the emission intensity for the complex Pt(5,5′-dimethyl-2,2′-bipyridine)$(CN)_2$ [8a]. Other researchers have reported similar self-quenching for related square planar platinum complexes, as well as the observation of weak excimer emission at high platinum complex concentrations [8,9]. The self-quenching mechanism used to explain this concentration dependent quenching process involves initial formation of the excited complex, M^*, followed by association with a ground state complex to give a weakly emissive excimer, $[M, M]^*$. The latter process is clearly dependent on the concentration of the metal complex. The model is identical to one used to describe the monomer/excimer fluorescence kinetics of aromatic hydrocarbons [10]. Using this model, the diffusion controlled self-quenching rate constants have been determined for a number of platinum complexes by monitoring the self-quenching reactions of the Pt complex as a function of concentration. Direct characterization of these platinum excimers, however, has been less documented due to limited solubility of the complexes, as well as weak emission and short lifetimes for the excimers [9].

Metal complexes in their excited states may be potent oxidizing and reducing agents [11], making them potentially useful as sensitizers for photochemical energy conversion (i.e. solar energy conversion). In this context, it is important to know the redox properties of excited metal complex, in order to design the optimal combination of donor and acceptor materials to interact with the sensitizer in a solar cell configuration. Likewise, in organic light-emitting diodes, a good understanding of the excited state redox properties is also important, since such knowledge will enable the best materials to be chosen in order to eliminate luminescent quenching by electron transfer between the excited dopant and the other materials in the device, processes that lead to a decreased OLED efficiency.

In this paper, we present a number of photophysical studies of **FPt** in solution at room temperature. The concentration dependent luminescent behavior of **FPt** was studied by static and transient spectroscopy. The **FPt** complex was found to undergo luminescent self-quenching at near diffusion controlled rates from monomer/excimer phosphorescence kinetic analysis. Energy transfer and electron transfer quenching studies of the complex **FPt** were also carried out to estimate the redox properties of the **FPt** ground and excited state [12].

2. Experimental

2.1. Materials

All of the neutral organic quenchers used here were commercially available and used as received. The pyridinium salts were prepared by refluxing the corresponding substituted pyridine with appropriate alkylating reagent in an acetone–methanol mixture overnight, followed by metathesis in water with NH_4PF_6. The solvent 2-methyltetrahydrofuran (2-MeTHF) was distilled under N_2 after being refluxed over sodium prior to use. The acetonitrile used was EM Science DriSolv solvent and used as received. **FPt** was prepared by a literature procedure [5].

2.2. Physical measurements

The UV–vis spectra were recorded on an Aviv model 14DS spectrophotometer (a re-engineered Cary 14 spectrophotometer). Photoluminescent spectra were measured using a Photon Technology International fluorimeter. Emission lifetime measurements were performed using time-correlated single photon counting on an IBH Fluorocube instrument. Samples were excited with 405 nm pulsed diode laser having a pulse duration of ca. 1.2 ns and an energy of 500 nJ/pulse. The energy per laser pulse was adequate to provide a transient signal yet low enough to prevent formation of high concentrations of excited state species, which would lead to quenching by triplet–triplet annihilation. The measured lifetimes have an error of 5%.

Quantum efficiency measurements were carried out at room temperature in a 2-methyltetrahydrofuran solution. Before spectra were measured, the solution was degassed by several freeze–pump–thaw cycles using a diffusion pump. Solutions of coumarin-47 in ethanol ($\Phi = 0.60$) were used as a reference. The equation $\Phi_s = \Phi_r(\eta_s^2 A_r I_s / \eta_r^2 A_s I_r)$ was used to calculate quantum yields, where Φ_s is the quantum yield of the sample, Φ_r is the quantum yield of the reference, η is the refractive index of the solvent, A_s and A_r are the ab-

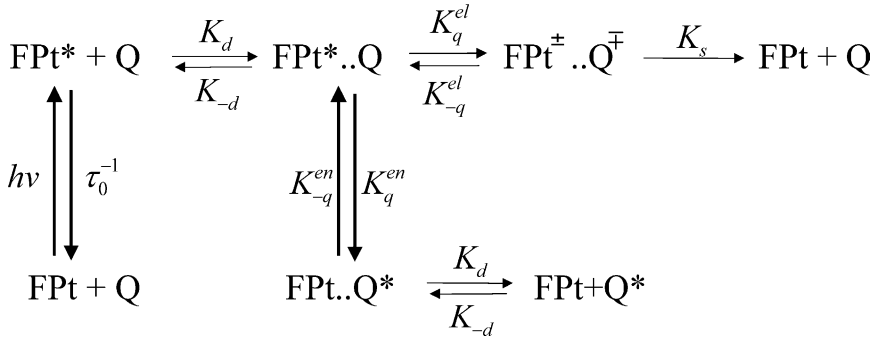

Scheme 1.

sorbance of the sample and the reference at the wavelength of excitation, and I_s and I_r are the integrated areas of emission bands.

Cyclic voltammetry and differential pulsed voltammetry were performed using an EG&G potentiostat/galvanostat model 283. Anhydrous DMF (Aldrich) was used as the solvent under a nitrogen atmosphere, and 0.1 M tetra(*n*-butyl)ammonium hexafluorophosphate was used as the supporting electrolyte. A Pt wire acted as the counter electrode, an Ag wire was used as the pseudo reference electrode, and the working electrode was glassy carbon. The redox potentials are based on values measured from differential pulsed voltammetry and are reported relative to an internal ferrocenium/ferrocene (Cp_2Fe^+/Cp_2Fe, 0.45 V versus SCE) [13] reference. Electrochemical reversibility was determined using cyclic voltammetry.

For the bimolecular quenching experiments, **FPt** concentration was set as 0.01 mM and the concentrations of quenchers were from 0 to 50 mM. Before each lifetime measurement, the solution samples were degassed by several freeze–pump–thaw cycles using a diffusion pump. In the case of oxidative quenching studies, the samples in acetonitrile were bubble degassed with dry argon for 15–30 min. A Stern–Volmer quenching analysis, as in Eq. (1), was applied to determine the bimolecular quenching rate constants, where I_0 and τ_0 are the emission intensity and excited state lifetime in absence of quenchers, I and τ are the corresponding values with the quenchers present, K_q is the experimental quenching rate constant and [Q] is the molar concentration of the quencher. For the self-quenching studies, the emission lifetimes in different concentrations were measured and the self-quenching rate K_q was determined using Eq. (2), where [FPt] is the total concentration of **FPt**.

$$\frac{I_0}{I} = \frac{\tau_0}{\tau} = 1 + K_q\tau_0[\mathrm{Q}] \tag{1}$$

$$\frac{\tau_0}{\tau} = 1 + K_q\tau_0[\mathrm{FPt}] \tag{2}$$

2.3. Data analysis for bimolecular quenching

The kinetics for electron transfer or energy transfer (shown in Scheme 1) has been modeled and can be fit with the following equations [12].

$$K_q^{el} = \frac{K_d}{1 + (K_{-d}/K_s)\exp(\Delta G_{el}/RT) + (K_{-d}/K_{el}^0)\exp(\Delta G_{el}^{\neq}/RT)} \quad \text{(electron transfer quenching)} \tag{3}$$

$$K_q^{en} = \frac{K_d}{1 + \exp(\Delta G_{en}/RT) + (K_{-d}/K_{en}^0)\exp(\Delta G_{en}^{\neq}/RT)} \quad \text{(energy transfer quenching)} \tag{4}$$

where $\Delta G_{en(el)}^{\neq} = \Delta G_{en(el)} + (\Delta G_{en(el)}^{\neq}(0)/\ln 2)\ln[1 + \exp(-\Delta G_{en(el)}\ln 2/\Delta G_{en(el)}^{\neq}(0))]$ (the free energy of activation: Agmon–Levine relationship) [14].

In these equations, the diffusion rate constant K_d and dissociation rate constant K_{-d} were determined as $K_d = 1.3 \times 10^{10}\,M^{-1}\,s^{-1}$ and $K_{-d} = 1.5 \times 10^{10}\,M^{-1}\,s^{-1}$ for the solvent 2-Me-THF and $K_d = 1.9 \times 10^{10}\,M^{-1}\,s^{-1}$ and $K_{-d} = 2.1 \times 10^{10}\,M^{-1}\,s^{-1}$ for the solvent acetonitrile at room temperature [15]. $K_{en(el)}^0$, $\Delta G_{en(el)}^{\neq}(0)$, and K_s are the pre-exponential factor, the reorganizational intrinsic barrier and rate constant for back electron transfer to form the reactants in their ground state, respectively. These values can be determined based on quenching studies done with closely related compounds and were chosen as $K_{en(el)}^0 \approx 1.4 \times 10^{10}\,s^{-1}$ and $\Delta G_{en(el)}^{\neq}(0) \approx 0.1$ eV to achieve the best fits to the experimental results and fall close to the values reported for closely related Pt complexes [12]. In electron transfer quenching, K_s was taken to equal K_{-d} [16]. The standard free energy change for energy transfer, ΔG_{en}, is given by the following equation: $\Delta G_{en} = -\{E^{00}([\mathrm{Pt}]^*, [\mathrm{Pt}]) - E^{00}(Q^*, Q)\}$, where E^{00} is the energy of the excited state derived from spectra for **FPt** and quenchers. The standard free energy change for electron transfer, ΔG_{el}, is given by $\Delta G_{el} = (E_{ox} - E_{red}) - E^{00} + W_p - W_r$, in which E_{ox} is the oxidation potential of the electron donor, E_{red} is the reduction potential of the electron acceptor, W_p and W_r are the work terms, which take the value of $W_p - W_r = 0.15$ eV for reductive electron transfer quenching [17] and have a negligible value for oxidative electron transfer quenching [25].

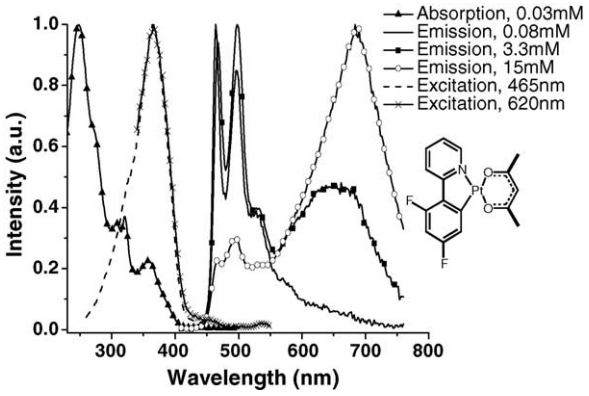

Fig. 1. Absorption, emission and excitation spectra of **FPt** at different concentrations in 2-MeTHF. The inset shows the molecular structure of **FPt**.

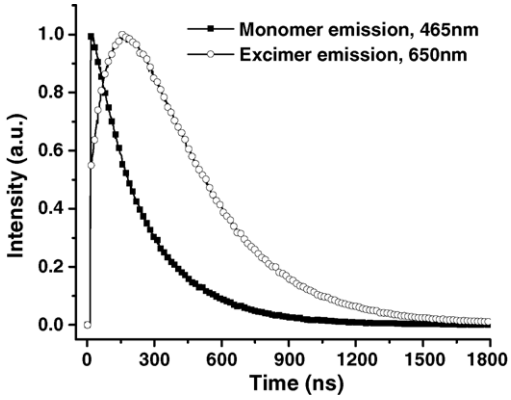

Fig. 2. Excited state decay curves of 0.25 mM **FPt** in 2-MeTHF monitored at 465 and 650 nm.

3. Results and discussion

3.1. Self-quenching

The absorption spectrum along with the room temperature luminescence spectra of **FPt** in 2-MeTHF at three different concentrations is shown in Fig. 1. Low energy transitions in the absorption spectrum (300–450 nm) are assigned as metal-to-ligand charge transfer (MLCT) transitions, while higher energy transitions (230–300 nm) are assigned to π–π^* ligand centered (LC) transitions. At low concentration, a vibronically structured luminescence (λ_{max} = 465 nm) is observed from a single emissive species. This emission has been previously assigned to phosphorescence from a triplet ligand centered (^{3}LC) state of the cyclometalated ligand that is strongly perturbed by mixing with a higher energy, singlet metal-to-ligand charge transfer (^{1}MLCT) state [5]. As the **FPt** concentration increases, a broad, low energy emission band (λ_{max} = 650 nm) grows into the spectrum, whereas dilution of the sample eliminates the low energy emission band. The absorption spectra of the dilute and concentrated samples are the same, having a lowest energy triplet absorption transition at 460 nm ($\varepsilon = 40\ M^{-1}\ cm^{-1}$) at room temperature. Excitation spectra recorded by monitoring emission wavelengths of 465 and 620 nm are identical (Fig. 1), and match the low energy absorption bands for **FPt**. Upon cooling a concentrated solution to 77 K, the 650 nm emission disappears and the higher energy emission increases in intensity and undergoes a small rigidochromic blue shift to 458 nm [5]. A vibronic progression is observed in the spectra at 77 K with a spacing of 1470 cm^{-1}. On the basis of this spectroscopic data, the structured high energy emission can be assigned to the **FPt** monomer and the featureless low energy emission band can be assigned to an **FPt** excimer. The time dependence of the emission intensity from the **FPt** monomer and excimer were measured by monitoring the luminescence decay at 465 and 650 nm, respectively (Fig. 2). Whereas the monomer signal shows emission decay commencing immediately after the excitation pulse, the excimer emission initially increases and then decays, consistent with initial formation of the excimer followed by its return back to the ground state.

The kinetics for the photophysics of an **FPt** solution can be treated as shown in Scheme 2 [9,10]. Here, K_q^M represents the monomer self-quenching rate constant (also the rate constant for excimer formation), K_d^M represents the decay rate for the monomer, and K_d^E is the decay rate for the excimer. A similar model has been successfully applied to treat monomer/excimer emission from both pyrene [10] and square planar platinum complexes [9]. The monomer emission intensity $i_M(t)$ and the excimer emission intensity $i_E(t)$ can then be described using Eqs. (5) and (6) respectively, where λ_1 and λ_2 are decay constants that are related to the rate parameters in the manner shown in Eq. (7). In this model, the large energy difference between the monomer and excimer (roughly 0.76 eV) makes the excimer extremely stable towards dissociation back to **FPt*** and **FPt**. Therefore, it can be assumed that the rate constant for excimer dissociation, K_s^E, is significantly smaller than K_q^M and thus, K_s^E can be neglected. This assumption leads to $(K_d^E + K_s^E - K_d^M - K_q^M[FPt]) \gg \sqrt{4K_q^M K_s^E[FPt]}$ at low to modest concentrations solutions ($\leq$3 mM). The decay constant, λ_1, can then be approximated as $\lambda_1 = K_d^M + K_q^M[FPt]$, i.e. the observed monomer decay rate at a given solution concentration, and the decay constant λ_2 can be treated approximately as $\lambda_2 = K_d^E$, i.e. the excimer decay rate.

$$i_M(t) \propto e^{-\lambda_1 t} + Ae^{-\lambda_2 t} \quad (5)$$

$$i_E(t) \propto e^{-\lambda_1 t} - e^{-\lambda_2 t} \quad (6)$$

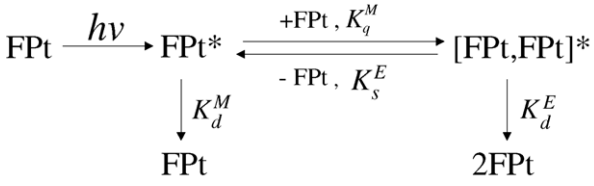

Scheme 2.

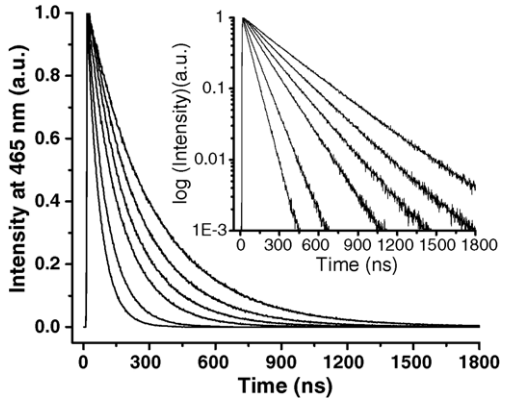

Fig. 3. Monomer luminescence decay curves for **FPt** in 2-MeTHF at concentrations listed in inset of Fig. 4. The inset shows the decay curves in a semilog plot.

where $A = (K_d^M + K_q^M[FPt] - \lambda_1)/(\lambda_2 - K_d^M + K_s^E[FPt])$, and

$$\lambda_{1,2} = \frac{1}{2}\left(K_d^M + K_q^M[FPt] + K_d^E + K_s^E \mp \sqrt{(K_d^E + K_s^E - K_d^M - K_q^M[FPt])^2 + 4K_q^M K_s^E[FPt]}\right) \quad (7)$$

The luminescent decay of **FPt** monomer at $\lambda_{max} = 465$ nm was examined at a number of different concentrations (Fig. 3). According to the model shown above, monomer emission decay should exhibit bi-exponential kinetics. However, our experimental results display a simple mono-exponential decay for the monomer at all concentrations studied (Fig. 3, inset), which can be simply explained as due to the pre-exponential factor, A, being $\ll 1$ (i.e. $K_s^E \ll K_q^M$). A plot of the measured emission decay rate versus the **FPt** concentration is linear (Fig. 4), matching the expected dependence, i.e. $K_{obs} = K_d^M + K_q^M[FPt]$. The slope of the linear fit to this data gives a large, near diffusion controlled self-quenching rate constant of $4.2 \pm 0.3 \times 10^9\ M^{-1}\ s^{-1}$ for excimer formation. This finding supports the assumption that K_s^E is quite small relative to K_q^M. The intercept of the linear fit to the data gives the emission rate in the absence of self-quenching (i.e. infinite dilution limit [FPt] ~ 0) and thus, an estimate of the intrinsic lifetime (τ_{rad}) for **FPt**. The intercept of the best-fit line ($K_d^M = 3.0 \times 10^6\ s^{-1}$) corresponds to an **FPt** monomer lifetime of 330 ns ($\pm$15 ns) at infinite dilution. A quantum efficiency of 0.6% was measured for **FPt** emission for a dilute sample (0.01 mM) where only monomer emission is observed. The radiative and non-radiative rate constants are then calculated to be $1.8 \times 10^4\ s^{-1}$ ($\tau_{rad} = 55\ \mu s$) and $3.0 \times 10^6\ s^{-1}$, respectively [18]. The radiative rate constants observed for **FPt** are similar to values reported for related square planar platinum complexes [9].

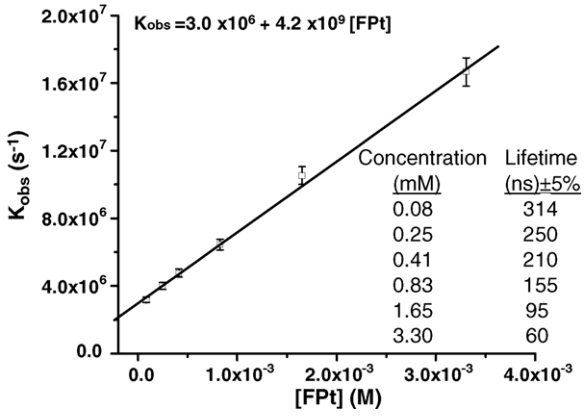

Fig. 4. Modified Stern–Volmer plot of self-quenching (squares) for **FPt**. The inset is a table of monomer lifetimes and concentrations.

Several groups have described excimer formation during self-quenching of platinum complexes [9]. Although the intrinsic monomer lifetimes and the self-quenching rate constants have been determined for most of the complexes through analysis of monomer luminescent self-quenching, few studies have determined the excimer emission decay rate directly [9b,f,i]. Fortunately, the **FPt** complex has sufficient solubility and high enough excimer luminescent efficiency to allow for direct measurement of the excimer formation and decay kinetics. The rise and fall of the excimer emission intensity in a 0.25 mM **FPt** solution was monitored at 650 nm. The excimer decay can be well fit with a bi-exponential function, representing the formation and decay of the excimer (Fig. 2). According to discussion above, the decay constant (λ_2) at such a concentration can be treated as equal to the excimer decay rate, K_d^E. Application of Eq. (6) to the excimer signal at 650 nm then gives K_d^E a value of $7.5 \pm 0.5 \times 10^6\ s^{-1}$ and thus, an excimer lifetime at ca. 135 ± 10 ns. Therefore, the **FPt** complex has comparable monomer (330 ± 15 ns) and excimer (135 ± 10 ns) lifetimes, which causes the pronounced rise and decay signals for the excimer emission intensity (Fig. 2). The monomer and excimer lifetimes for **FPt** are similar to those of other Pt complexes reported in the literature, although there is a wide spread in excimer lifetimes (40–3000 ns) [9i]. Some platinum complexes, e.g. Pt(4,4′-di-*tert*-butylbipyridine)$(CN)_2$, have monomer and excimer lifetimes that differ by a factor of 100 ($\tau_{monomer} = 2900$ ns; $\tau_{excimer} \approx 40$ ns) [9b]. Unfortunately, it is not possible to determine a value for the quantum efficiency for excimer emission, so the radiative and non-radiative rates for the two types of emissive species cannot be compared.

While we have focused on the solution photophysical properties of **FPt**, D'Andrade and Forrest have examined the excimer formation and decay kinetics for **FPt** in the solid state in both neat and doped thin films [7d]. Both **FPt** monomer and excimer emission were observed under these conditions

at room temperature and 10 K, with the proportion of emission from the monomer increasing with decreasing temperature. The behavior is consistent with only a small fraction of the **FPt** molecules being in the appropriate disposition to generate excimer emission upon excitation of individual **FPt** molecules. Energy from an **FPt*** molecule in the solid state migrates via exciton diffusion through the lattice by intermolecular energy transfer before being trapped by an **FPt** "excimeric" dimer, as opposed to the situation in fluid solution, where excimer formation occurs by physical diffusion of an **FPt*** molecule. In a neat **FPt** film, the lifetime of monomeric emission ($\lambda = 470$ nm) decreases from $\tau = 8.7$ μs at 5 K to $\tau = 250$ ns at 220 K [7d]. Exciton quenching of **FPt*** at a relatively small number of excimer sites presumably contributes to the decrease in lifetime with increasing temperature in the solid state. At higher temperatures, the **FPt*** exciton has a larger diffusion radius (due to thermally activated intermolecular energy transfer) and is more likely to encounter an excimer formation site prior to unimolecular decay. Since the processes for generating **FPt** excimer emission in solution and the solid state are very different, it is not proper to compare the parameters determined for the rates of excimer formation in the two systems. It is, however, useful to compare monomer and excimer decay rates in the two systems. In fluid solution, the room temperature lifetime of **FPt*** decreases from 330 ns at infinite dilution to 60 ns at a concentration of 3 mM. The low barrier for physical diffusion of **FPt*** in fluid solution leads to **FPt*** quenching by excimer formation at a markedly faster rate than does **FPt*** exciton trapping by "excimeric" dimers in the solid state. The lifetime for **FPt** excimer emission in the neat solid (corrected to eliminate the weak monomer contribution) is nearly temperature independent, decreasing from 1.7 μs at 100 K to 1.3 μs at 220 K. On the other hand, the **FPt** excimer lifetime measured in 0.25 mM solution is shorter (135 ns) and consistent with non-radiative decay channels being present in fluid solution that are inaccessible in the neat solid.

3.2. Excited state properties

3.2.1. Redox properties estimated from electrochemistry and spectra

Cyclic voltammetry of **FPt** shows a single reversible reduction at −2.29 V versus Cp_2Fe^+/Cp_2Fe (−1.84 V versus SCE) and an irreversible oxidative wave at 0.52 V versus Cp_2Fe^+/Cp_2Fe (0.97 V versus SCE) [5]. The reduction is considered to be localized on the cyclometalated ligand while the oxidation is thought to occur predominantly at the metal center [5]. Oxidation of square planar Pt^{II} complexes is typically irreversible due to rapid solvolysis of the resultant Pt^{III} species [19]. While differential solvation of the cationic and anionic forms of **FPt** may affect the potentials measured here, the difference in oxidation and reduction potentials, 2.81 eV, can be used as an estimate of the HOMO–LUMO energy gap. An alternate method for evaluating the HOMO–LUMO separation is to use low energy edge of the ^{1}MLCT transition in the absorption spectrum of **FPt** (Fig. 1), which occurs at 3.1 eV (∼400 nm). This spectroscopic method for estimating the HOMO–LUMO gap may also give an inaccurate value, due to solvation, correlation and reorganization effects, thus both electrochemical and spectroscopic methods should be treated as estimates [20]. The difference of ca. 0.3 eV between the two estimates of the HOMO–LUMO energy gap for **FPt**, combined with the irreversible nature of the electrochemical oxidation process, creates considerable uncertainty in the value of the thermodynamic oxidation potential of **FPt**. Fortunately, a thermochemical cycle (Scheme 3) can be constructed to estimate the ground state redox potentials from the excited state redox properties and the luminescence data. Therefore, in order to gain a more quantitative picture of the ground and excited state energetics, a number of bimolecular quenching studies were carried out with the **FPt** complex.

3.2.2. Energy transfer quenching

A range of organic molecules with different triplet energies were used as triplet energy transfer quenchers in this

Table 1
Rate constants for energy transfer quenching of **FPt**

Triplet quenchers	$E(D^+/D)$[a]	$E(A^+/A)$[b]	E_T (eV)[c]	ΔG (eV)[d]	K_q (M^{-1} s^{-1})[e]
Anthracene	1.16	−1.93	1.85	−0.86	7.22×10^9
trans-Stilbene		−2.26	2.12	−0.59	5.75×10^9
1-Cyanonaphthalene		−1.98	2.49	−0.22	5.96×10^9
2-Methoxynaphthalene	1.42		2.62	−0.09	3.72×10^9
Naphthalene	1.60	−2.29	2.64	−0.07	4.23×10^9
Phenanthrene	1.58	−2.20	2.69	−0.02	2.66×10^9
Triphenylene	1.64	−2.22	2.89	0.18	6.66×10^7
Fluorene	1.55		2.94	0.23	2.99×10^7
Methyl-*p*-cyanobenzoate		−1.76	3.12	0.41	$<10^6$

[a] Oxidation potential (vs. SCE, values from [12a]).
[b] Reduction potential (vs. SCE, values from [12a]).
[c] Triplet energy (values from [12a]).
[d] Free energy change for energy transfer (values calculated using $E^{00} = 2.71$ eV).
[e] Bimolecular quenching rate constant.

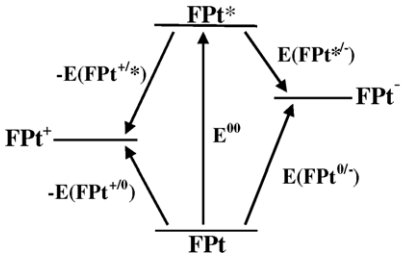

Excited state reduction potential: $E(FPt^{*/-}) = E^{00} + E(FPt^{0/-})$

Excited state oxidation potential: $-E(FPt^{+/*}) = E^{00} - E(FPt^{+/0})$

Scheme 3.

study (Table 1). The redox properties of the chosen quenchers make electron transfer unlikely, based on a preliminary estimate of the excited state redox properties of **FPt**. The rate constants for energy transfer quenching by each of the quenchers were determined from the slopes of the Stern–Volmer plots and are listed in Table 1. A semilog plot of K_q^{en} versus E_T (the triplet energy of a given quencher) shows a marked dependence of the quenching rate on the triplet energy of the quencher (Fig. 5a). Using the kinetic analysis discussed in the experimental section, the best fit to the experimental energy transfer quenching data gives an E^{00} value of 2.80 eV. The triplet energy of **FPt** obtained in this way is very close to the E^{00} value of 2.71 eV determined using the highest energy emission peak in a 2-MeTHF solution at 77 K (458 nm) [21]. This study also emphasizes the importance of using high triplet energy host materials in order to prevent luminescent quenching by energy transfer and thereby maximize efficiencies in phosphor-doped OLEDs [22].

3.2.3. *Reductive electron transfer quenching*

Amines have proven to be excellent reductive electron transfer quenchers in the studies of Pt complex excited states [23]. The high triplet energies of these amines, as well as their high reduction potentials (Table 2), make both energy transfer and oxidative electron transfer quenching of the **FPt** excited state unfavorable. The reductive quenching rate constants (from Stern–Volmer analysis) for each of the amines are given in Table 2 and plotted in Fig. 5b versus the oxidation potential of each quencher. Increasing the oxidation potential of the quencher leads to a pronounced decrease in the reductive quenching rate. Applying the model for electron transfer quenching discussed in the experimental section, the best fit to the experimental data for the excited-state reduction potential is 0.81 V versus SCE. This value is very close to one estimated from the E^{00} energy and the ground state reduction potential using Scheme 3 (0.87 V versus SCE). This is to be expected, since the reduction is completely reversible and the phosphorescence energy is similar to the triplet energy determined in the quenching studies.

The effects of both energy transfer and electron transfer quenching need to be considered when employing **FPt** as the dopant in OLEDs. Since **FPt** has a high triplet energy and a high excited-state oxidation potential, an appropriate host material should exceed both parameters to maximize the luminescent efficiency of a device. A good demonstration of the problem is seen for mixtures of **FPt** and *N*,*N*′-diphenyl-*N*,*N*′-di(3-toly)benzidine (TPD), a common hole transporter for OLEDs. TPD has a triplet energy of 2.3 eV and an oxidation potential of 0.73 V versus SCE. As shown in Fig. 6, thin films of TPD doped with 1 wt.% **FPt** do not show any monomer

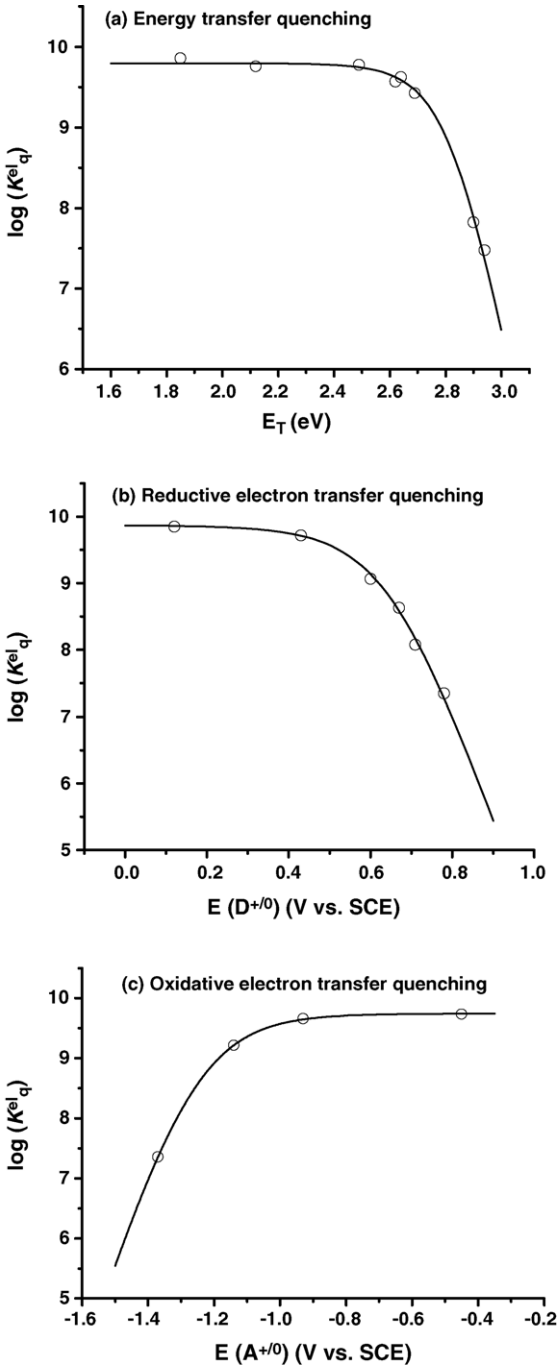

Fig. 5. Plots of the $\log(K_q^{en(el)})$ vs. E_T (Q*, Q), $E_{1/2}^{Oxi}$ and $E(A^{+/0})$ for energy transfer quenching (a), reductive electron transfer quenching (b) and oxidative electron transfer quenching (c) of **FPt***, respectively, by organic molecules in 2-MeTHF at room temperature. Circles represent experimental data, solid lines are best fitting curves.

Table 2
Rate constants for reductive electron transfer quenching of **FPt**

Reductive quenchers	$E(D^+/D)$ (V)[a]	E_T (eV)[b]	K_q (M^{-1} s^{-1})[c]
N,*N*,*N*′,*N*′-Tetramethyl-1,4-benzenediamine	0.12		10.6×10^9
N,*N*,*N*′,*N*′-Tetramethylbenzidine	0.43	2.73	8.21×10^9
1,4-Diazabicyclo[2.2.2]octane	0.60	>3.9	1.16×10^9
N,*N*,*N*′,*N*′-Tetramethyldiaminoethane	0.67	>3.9	4.28×10^8
N,*N*-Dimethyl-*p*-toluidene	0.71	3.1	2.19×10^8
Triethylamine	0.78	>3.9	2.21×10^7

[a] Potential vs. SCE (values from [23]).
[b] Triplet energy (values from [12a]).
[c] Bimolecular quenching rate constant.

FPt emission, rather TPD fluorescence and **FPt** excimer-like emission are observed instead [24]. This quenching of the **FPt** monomer emission is to be expected when one considers the differences in electrochemical potentials and triplet energies between the two host materials. Reductive electron transfer reaction of **FPt** is spontaneous with a 0.08 V driving force, whereas energy transfer to TPD is exergonic by nearly 0.4 eV. On the other hand, the **FPt** excimer-like state in the doped TPD film is not quenched. The lower triplet energy, and consequently less positive excited-state oxidation potential, of the excimer are endogonic with respect to the TPD triplet state energy and reduction potentials. Hence, if **FPt** is doped into a material with a higher oxidation potential and higher triplet energy, such as CBP (CBP = 4,4′-*N*,*N*-dicarbazole-biphenyl, E_{oxid} = 0.98 V versus SCE, E_T = 2.6 eV), both **FPt** monomer and excimer-like luminescence are observed from doped thin films (see Fig. 6).

3.2.4. Oxidative electron transfer quenching

Pyridinium acceptors have previously been used for oxidative quenching experiments [25]. These compounds have both high triplet energies and oxidation potentials [26], precluding energy transfer or reductive quenching processes from occurring with most donor compounds. The quenching rate constants of $\mathbf{FPt}^*$ by these pyridinium quenchers are

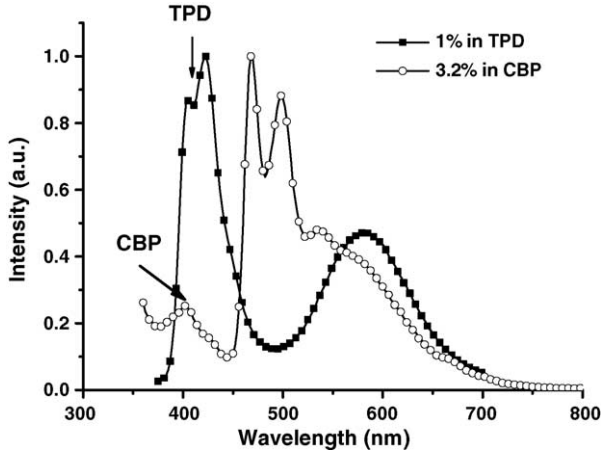

Fig. 6. Photoluminescence spectra of ∼1% **FPt** doped into TPD and 3.2% **FPt** doped into CBP.

Table 3
Rate constants for oxidative electron transfer quenching of **FPt**

Oxidative quenchers[a]	$E(A^+/A)$ (V)[b]	K_q (M^{-1} s^{-1})[c]
N,*N*′-Dimethyl-4,4′-pyridinium	−0.45	5.42×10^9
4-Amido-*N*-ethylpyridinium	−0.93	4.56×10^9
3-Amido-*N*-methylpyridinium	−1.14	1.63×10^9
N-Ethylpyridinium	−1.37	2.28×10^7

[a] Hexafluorophosphate salts.
[b] Potential vs. SCE (values from [25]).
[c] Bimolecular quenching rate constant.

presented in Table 3. A plot of log K_q^{el} versus $E(A^{+/0})$ for the oxidative quenching is shown in Fig. 5c. The curve shown in Fig. 5c is the best fit to the experimental data using Eq. (3) and gives an excited-state oxidation potential of −1.41 V versus SCE. In the fitting process used here, the only parameter being adjusted to achieve the best fit is the excited-state oxidation potential (see previous discussion). Application of the thermochemical cycle in Scheme 3 gives a value of 1.30 V versus SCE for the ground state oxidation potential of **FPt**. This value calculated from the excited-state reduction potential, when combined with the reversible reduction potential of −1.84 V versus SCE determined by cyclic voltammetry, gives a HOMO–LUMO energy gap in 3.14 eV. The energy of the HOMO–LUMO gap (395 nm) obtained in this manner closely corresponds to the onset of the ^{1}MLCT transition in the absorption spectrum. Therefore, we can conclude that thermodynamic ground state oxidation potential for **FPt** is nearer 1.30 V versus SCE, rather than the value of 0.97 V versus SCE obtained using electrochemical methods.

4. Conclusions

We have conducted a series of luminescent quenching studies of the molecule **FPt** in solution phase at room temperature. The formation of red shifted emissive phosphorescent triplet excimers from the self-quenched triplet excited state monomers has been observed in 2-MeTHF solution at room temperature. A rate constant of $4.2 \pm 0.3 \times 10^9$ M^{-1} s^{-1} for the excimer formation has been determined from the monomer self-quenching behavior. The intrinsic lifetime for the excited state of the monomer was determined to be 330 ns

(±15 ns) at infinite dilution, while the excimer lifetime was found to be ca. 135 ns (±10 ns) for a 0.25 mM solution.

Energy transfer and electron transfer quenching studies were carried out to determine the photoredox properties of excited state of the **FPt** complex. Values obtained for the triplet energy (2.80 eV) and the excited-state reduction potential (0.81 V versus SCE) from these studies are in accord with values estimated using the E^{00} energy from the emission spectra and a thermodynamic cycle (Scheme 3) based on the electrochemical and spectral properties of the **FPt** complex. An excited-state reduction potential of −1.41 V versus SCE was also obtained by an oxidative electron transfer quenching study. This value does not concur with the value predicted from electrochemical and spectroscopic measurements due to the irreversibility of the electrochemical oxidation. However, using the thermodynamic cycle and the E^{00} energy from the emission spectrum, the ground state oxidation potential for **FPt** is estimated to be near 1.30 V versus SCE. This value for the oxidation potential of **FPt** is a consistent with the value calculated using the onset of the ^{1}MLCT transition and the reversible reduction potential of the complex. With a good picture of the excited state energy and redox properties in hand, we expect to be able to design OLEDs with higher efficiencies, as well as high efficiency solar cells, using **FPt** as the light emitter or absorber, respectively.

Acknowledgements

This work was supported by Universal Display Corp. and the National Science Foundation. We thank Dr. Jason Brooks, Dr. Bert Alleyne, Jian Li, and Arnold Tamayo for helpful discussions. Biwu Ma would like to thank USC School of Engineering for Dean's Fellowship support.

References

[1] (a) C.S. Peyratout, T.K. Aldridge, D.K. Crites, D.R. McMillin, Inorg. Chem. 34 (1995) 4484;
(b) A.H.-J. Wang, J. Nathans, G.A. Van Der Marel, J.H. Van Boom, A. Rich, Nature 276 (1978) 471;
(c) V.H. Houlding, A.J. Frank, Inorg. Chem. 24 (1985) 3664;
(d) T. Maruyama, T. Yamamoto, J. Phys. Chem. B 101 (1997) 3806;
(e) V. Anbalagan, T.S. Srivastava, J. Photochem. Photobiol. A: Chem. 89 (1995) 113.

[2] (a) D.M. Roundhill, H.B. Gray, C.M. Che, Acc. Chem. Res. 22 (1989) 55;
(b) D.G. Nocera, Acc. Chem. Res. 28 (1995) 209;
(c) W. Paw, S.D. Cummings, M.A. Mansour, W.B. Connick, D.K. Geiger, R. Eisenberg, Coord. Chem. Rev. 171 (1998) 125.

[3] (a) M. Hissler, J.E. McGarrah, W.B. Connick, D.K. Geiger, S.D. Cummings, R. Eisenberg, Coord. Chem. Rev. 208 (2000) 115;
(b) J.E. McGarrah, Y.-J. Kim, M. Hissler, R. Eisenberg, Inorg. Chem. 40 (2001) 4510;
(c) E.M. James, R. Eisenberg, Inorg. Chem. 42 (2003) 4355.

[4] (a) M.A. Baldo, D.F. O'Brien, Y. You, A. Shoustikov, S. Sibley, M.E. Thompson, S.R. Forrest, Nature 395 (1998) 151;
(b) R.C. Kwong, S. Sibley, T. Dubovoy, M.A. Baldo, S.R. Forrest, M.E. Thompson, Chem. Mater. 11 (1999) 3709;
(c) D.R. O'Brien, M.A. Baldo, M.E. Thompson, S.R. Forrest, Appl. Phys. Lett. 74 (1999) 442;
(d) C. Adachi, M.A. Baldo, S.R. Forrest, S. Lamansky, M.E. Thompson, R.C. Kwong, Appl. Phys. Lett. 78 (2001) 1622;
(e) V. Cleave, G. Yahioglu, P.L. Barny, R.H. Friend, N. Tessler, Adv. Mater. 11 (1999) 285;
(f) Y. Kunugi, K.R. Mann, L.L. Miller, C.L. Exstrom, J. Am. Chem. Soc. 120 (1998) 589;
(g) S.-C. Chan, M.C. Chan, Y. Wang, C.M. Che, K.K. Cheung, N. Zhu, Chem. Eur. J. 7 (2001) 4180;
(h) W. Lu, B.X. Mi, M.C.W. Chan, Z. Hui, N. Zhu, S.T. Lee, C.M. Che, Chem. Commun. (2002) 206.

[5] J. Brooks, Y. Babayan, S. Lamansky, P.I. Djurovich, I. Tsyba, R. Bau, M.E. Thompson, Inorg. Chem. 41 (2002) 3055.

[6] (a) M.A. Baldo, D.F. O'Brien, M.E. Thompson, S.R. Forrest, Phys. Rev. B 60 (1999) 14422;
(b) M.A. Baldo, S. Lamansky, P.E. Burrows, M.E. Thompson, S.R. Forrest, Appl. Phys. Lett. 75 (1999) 4;
(c) C. Adachi, M.A. Baldo, S.R. Forrest, M.E. Thompson, Appl. Phys. Lett. 77 (2000) 904;
(d) M. Ikai, S. Tokito, Y. Sakamoto, T. Suzuki, Y. Taga, Appl. Phys. Lett. 79 (2001) 156.

[7] (a) B. D'Andrade, M.E. Thompson, S.R. Forrest, Adv. Mater. 14 (2002) 147;
(b) B. D'Andrade, J. Brook, V. Adamovich, M.E. Thompson, S.R. Forrest, Adv. Mater. 14 (2002) 1032;
(c) V. Adamovich, J. Brooks, A. Tamayo, A.M. Alexander, P.I. Djurovich, B.D. Andrade, C. Adachi, S.R. Forrest, M.E. Thompson, New J. Chem. 9 (2002) 1171;
(d) B. D'Andrade, S.R. Forrest, J. Chem. Phys. 286 (2003) 321.

[8] (a) C.M. Che, K.T. Wan, L.Y. He, C.K. Poon, V.W.-W. Yam, J. Chem. Soc., Chem. Commun. (1989) 943;
(b) C.W. Chan, C.M. Che, M.C. Cheng, Y. Wang, Inorg. Chem. 31 (1992) 4874;
(c) W.B. Connick, H.B. Gray, J. Am. Chem. Soc. 119 (1997) 11620.

[9] (a) H. Kunkely, V. Vogler, J. Am. Chem. Soc. 112 (1990) 5625;
(b) K.-T. Wan, C.M. Che, K.C. Cho, J. Chem. Soc., Dalton Trans. (1991) 1077;
(c) C.W. Chan, T.F. Lai, C.M. Che, S.M. Peng, J. Am. Chem. Soc. 115 (1993) 11245;
(d) H.K. Yip, K.K. Cheng, S.M. Peng, C.M. Che, J. Chem. Soc., Dalton Trans. (1993) 2933;
(e) C.N. Pettijohn, E.B. Jochnowitz, B. Chuong, J.K. Nagle, A. Vogler, Coord. Chem. Rev. 171 (1998) 85;
(f) W.B. Connick, D. Geiger, R. Eisenberg, Inorg. Chem. 38 (1999) 3264;
(g) M. Hissler, W.B. Connick, D.K. Geiger, J.E. McGarrah, D. Lipa, R.J. Lachicotte, R. Eisenberg, Inorg. Chem. 39 (2000) 447;
(h) M. Hissler, J.E. McGarrah, W.B. Connick, D.K. Geiger, S.D. Cummings, R. Eisenberg, Coord. Chem. Rev. 208 (2000) 115;
(i) W.L. Fleeman, W.B. Connick, Comments Inorg Chem. 23 (2002) 205;
(j) J.A.G. Williams, A. Beeby, E.S. Davies, J.A. Weinstein, C. Wilson, Inorg. Chem. 42 (2003) 8609.

[10] (a) J.B. Birks, D.J. Dyson, I.H. Munro, Proc. R. Soc. A 275 (1963) 575;
(b) J.B. Birks, Photophysics of Aromatic Molecules, University of Manchester, 1970.

[11] D.M. Roundhill, Photochemistry and Photophysics of Metal Complexes, Plenum Press, New York, 1994, p. 17.

[12] (a) J.K. George, N.J. Turro, Chem. Rev. 86 (1986) 401, and reference therein;
(b) V. Balzani, F. Bolletta, F. Scandola, J. Am. Chem. Soc. 102 (1980) 2152;
(c) B. Marciniak, G.L. Hug, Coord. Chem. Rev. 159 (1997) 55, and reference therein.

[13] (a) R.R. Gagne, C.A. Koval, G.C. Lisensky, Inorg. Chem. 19 (1980) 2854;
(b) D.T. Sawyer, A. Sobkowiak, J.L. Roberts, Electrochemistry for Chemists, second ed., Wiley, New York, 1995, p. 467.
[14] (a) N. Agmon, R.D. Levine, Chem. Phys. Lett. 52 (1977) 197;
(b) N. Agmon, J. Chem. Soc., Faraday Trans. 74 (1978) 388.
[15] (a) J. Saltiel, B.W. Atwater, in: D.H. Volman, G.S. Hammond, K. Gollnick (Eds.), Advances in Photochemistry, vol. 14, Wiley, New York, 1988 ($K_d = 8000RT/3\eta$; Debye equation);
(b) M. Eigen, Z. Phys. Chem. (Leipzig) 203 (1954) 176 ($K_{-d} = K_d(3000/4\pi R^3 N_0)$, η is the solvent viscosity, R is the reaction radius (taken as 7×10^{-8} cm) and N_0 is the Avogadro number).
[16] (a) G.L. Hug, B. Marciniak, J. Phys. Chem. 98 (1994) 7523;
(b) F. Wilkinson, C. Tsiamis, J. Am. Chem. Soc. 105 (1983) 767;
(c) B. Marciniak, H.G. Lohmannsroben, Chem. Phys. Lett. 148 (1988) 29.
[17] (a) H. Knibbe, D. Rehm, A. Weller, B. Bunsenges, Phys. Chem. 72 (1968) 257;
(b) A.Z. Weller, Phys. Chem. (Wiesbaden) 133 (1982) 93.
[18] The radiative (k_r) and non-radiative (k_{nr}) rate constants are determined from the emission lifetime (τ) and quantum efficiency (ϕ_{em}) using the following equations: $k_r = \phi_{em} \times \tau^{-1}$ and $k_{nr} = k_r(\phi_{em}^{-1} - 1)$..
[19] P.I. Kvam, M.V. Puzyk, K.P. Balashev, J. Songstad, Acta Chem. Scand. 49 (1995) 335.
[20] A.B.P. Lever, E.S. Dodsworth, in: E.I. Solomon, A.B.P. Lever (Eds.), Inorganic Electronic Structure and Spectroscopy, vol. 2, Wiley, New York, 1999, p. 227.
[21] N.J. Turro, Modern Molecular Photochemistry, University Science Books, Sausalito, 1991.
[22] (a) M. Sudhakar, P.I. Djurovich, T.E. Hogen-Esch, M.E. Thompson, J. Am. Chem. Soc. 125 (2003) 7796;
(b) M.A. Baldo, S.R. Forrest, Phys. Rev. B 62 (2000) 10958.
[23] (a) J.M. Bevilacqua, R. Eisenberg, Inorg. Chem. 33 (1994) 1886;
(b) N. Kitamura, H.B. Kim, S. Okano, S. Tazuke, J. Phys. Chem. 93 (1989) 5750;
(c) D. Sandrini, M. Maestri, P. Belser, A. Von Zelewsky, V. Balzani, J. Phys. Chem. 89 (1985) 3675;
(d) C.R. Bock, J.A. Connor, A.R. Gutierrez, T.J. Meyer, D.G. Whitten, B.P. Sullivan, J.K. Nagle, J. Am. Chem. Soc. 101 (1979) 4815;
(e) B. Ballardini, G. Varani, M.T. Indelli, F. Scandola, V. Balzani, J. Am. Chem. Soc. 100 (1978) 7219;
(f) W. Hub, S. Schneider, F. Doerr, J.D. Oxman, F.D. Lewis, J. Am. Chem. Soc. 106 (1984) 701.
[24] J. Brooks, Ph.D. thesis, University of Southern California, 2002.
[25] (a) J.L. Marshall, S.R. Stobart, H.B. Gray, J. Am. Chem. Soc. 106 (1984) 3027;
(b) V.W. Yam, K.K. Lo, K.K. Cheung, Inorg. Chem. 35 (1996) 3459;
(c) C.M. Che, H.Y. Chao, V.M. Miskowski, Y. Li, K.K. Cheung, J. Am. Chem. Soc. 123 (2001) 4985;
(d) H.Y. Chao, W. Lu, Y. Li, C.W. Chan, C.M. Che, K.K. Cheung, N. Zhu, J. Am. Chem. Soc. 124 (2002) 14696.
[26] A. Ledwith, Acc. Chem. Res. 5 (1972) 133.